THE ASTROPHYSICAL JOURNAL, 599:L107–L110, 2003 December 20

HIGH-RESOLUTION INFRARED SPECTROSCOPY OF THE BROWN DWARF ϵ INDI Ba[1,2]

VERNE V. SMITH[3]
Department of Physics, University of Texas at El Paso, El Paso, TX 79968; verne@barium.physics.utep.edu
TAKASHI TSUJI
Institute of Astronomy, University of Tokyo, Mitaka, JP Tokyo 181, Japan; ttsuji@ioa.s.u-tokyo.ac.jp
KENNETH H. HINKLE
National Optical Astronomy Observatory,[4] P.O. Box 26732, Tucson, AZ 85726; khinkle@noao.edu
KATIA CUNHA[3]
Observatorio Nacional, Rua General Jose Cristino 77, Sao Cristovao, 20921-400 Rio de Janeiro, Brazil; katia@on.br
ROBERT D. BLUM[3]
Cerro Tololo Inter-American Observatory, 950 North Cherry Street, Tucson, AZ 85719; rblum@ctio.noao.edu
JEFF A. VALENTI
Space Telescope Science Institute, 3700 San Martin Drive, Baltimore, MD 21218; valenti@stsci.edu
STEPHEN T. RIDGWAY AND RICHARD R. JOYCE
National Optical Astronomy Observatory,[4] P. O. Box 26732, Tucson, AZ 85726; sridgway@noao.edu, rjoyce@noao.edu
AND
PETER BERNATH
Department of Chemistry, University of Waterloo, Waterloo, ON N2L 3G1, Canada; bernath@uwaterloo.ca
Received 2003 August 29; accepted 2003 November 10; published 2003 December 3

ABSTRACT

We report on the analysis of high-resolution infrared spectra of the newly discovered brown dwarf ϵ Ind Ba. This is the closest known brown dwarf to the solar system, with a distance of 3.626 pc. Spectra covering the ranges of $\lambda\lambda$2.308–2.317 μm and $\lambda\lambda$1.553–1.559 μm were observed at a resolution of $\lambda/\Delta\lambda = R = 50{,}000$. The physical parameters of effective temperature and surface gravity are derived for ϵ Ind Ba by comparison with model spectra calculated from atmospheres computed using unified cloudy models. The results are $T_{\rm eff} = 1500 \pm 100$ K, $\log g = 5.2 \pm 0.3$ (in units of cm s^{-2}), placing it in the critical boundary between the late L and early T dwarfs. The high spectral resolution also allows us to measure an accurate projected rotational velocity, with $v \sin i = 28 \pm 3$ km s^{-1}. Combined with a published luminosity for ϵ Ind Ba [with $\log (L/L_{\odot}) = -4.71$], the derived parameters result in a "spectroscopic" mass estimate of $\sim 30 M_{\rm J}$, a radius of $\sim 0.062\ R_{\odot}$, and a maximum rotational period of $\sim$3.0 hr. A compilation and comparison of effective temperatures derived from spectroscopy using model atmospheres versus those derived from luminosities and theoretical $M_{\rm bol}$-radius relations reveal a systematic disagreement in the $T_{\rm eff}$ scale. The source of this disagreement is unknown.

Subject headings: infrared: stars — stars: fundamental parameters — stars: individual (ϵ Indi B) — stars: low-mass, brown dwarfs

1. INTRODUCTION

The recently discovered nearby T-dwarf companion to ϵ Ind (Scholz et al. 2003) will be important in improving our understanding of the behavior of brown dwarfs that fall within the newly defined L and T spectral types (e.g., Kirkpatrick et al. 1999; Geballe et al. 2002). The T dwarf reported by Scholz et al. (2003) was discovered by Volk et al. (2003) and McCaughrean et al. (2003) to be a close optical double consisting of an early T dwarf (ϵ Ind Ba) and a late T dwarf (ϵ Ind Bb) separated by 0.″6. With an accurately known distance of 3.626 ± 0.009 pc, ϵ Ind Ba and Bb are the nearest known brown dwarfs. They share a common proper motion with the K5 V star ϵ Indi, lying at a projected distance of $\sim$1460 AU from their presumed primary star. The age of ϵ Ind itself has been estimated by Lachaume et al. (1999) to be $\sim$0.8–2.0 Gyr: this age estimate is based on its rotational velocity and Ca II K line emission. Thus, ϵ Ind Ba and Bb are brown dwarfs with very well defined luminosities and approximate ages.

We present the first high-resolution infrared (IR) spectroscopic observations of ϵ Ind Ba. Synthetic spectra computed from unified cloudy models by Tsuji (2002) are compared to the observed high-resolution spectra; these comparisons are used to derive the stellar parameters of effective temperature ($T_{\rm eff}$), surface gravity (defined as $\log g$), and projected rotational velocity ($v \sin i$).

2. OBSERVATIONS

High-resolution IR spectra were obtained on ϵ Ind Ba using the 8.1 m Gemini South reflecting telescope and the NOAO Phoenix spectrometer (Hinkle et al. 1998). This instrument is a cryogenically cooled echelle spectrograph that uses order-separating filters to isolate individual echelle orders. The detector is a 1024 × 1024 InSb Aladdin II array. The size of the detector in the dispersion direction limits the wavelength coverage in a single exposure to about 0.5% (1550 km s^{-1}, or

[1] Based on observations obtained at the Gemini Observatory, which is operated by the Association of Universities for Research in Astronomy, Inc., under a cooperative agreement with the NSF on behalf of the Gemini partnership: the National Science Foundation (United States), the Particle Physics and Astronomy Research Council (United Kingdom), the National Research Council (Canada), CONICYT (Chile), the Australian Research Council (Australia), CNPq (Brazil), and CONICRT (Argentina).

[2] Based on observations obtained with the Phoenix infrared spectrograph, developed and operated by the National Optical Astronomy Observatory.

[3] Visiting Astronomer, Gemini South Observatory.

[4] Operated by Association of Universities for Research in Astronomy, Inc., under cooperative agreement with the National Science Foundation.

~0.0120 μm at 2.3 μm and ~0.0080 μm at 1.6 μm). One edge of the detector is blemished, so the wavelength coverage on all but the brightest source is typically trimmed a few percent to avoid this area. The spectra discussed here were observed with the widest (0.″35) slit resulting in a spectral resolution of $R = \lambda/\Delta\lambda = 50{,}000$. Two spectral regions were observed, with one centered at $\lambda = 2.314$ μm and the other centered at 1.555 μm. These spectral regions sample crucial diagnostic lines from the molecules CO, H_2O, and CH_4.

At the time of our observations we were unaware of the existence of ϵ Ind Bb. Following the discovery (Volk et al. 2003; McCaughrean et al. 2003) we reexamined our acquisition images. Acquisition images of ϵ Ind B at 1.647 μm taken on 2003 August 13 under good conditions (0.″4 FWHM delivered image quality [DIQ]) confirm the Volk et al. (2003) detection. The companion can also be seen in 1.558 μm images on 2002 December 29, although it is less well resolved because of inferior seeing (0.″8 DIQ). It is, however, barely perceptible at 2.321 μm (2003 January 16) with 0.″4 DIQ. The issue relevant to the current investigation is the extent to which the spectrum of ϵ Ind Ba might suffer contamination from a nearby companion. The observed image profile at 1.647 μm is well fitted by a model in which the companion is fainter by 1.9 mag and is 0.″65 away at a position angle of 125°. At 2.321 μm the magnitude difference is greater than 3 between the two stars, so that the companion could contribute no more than 6% to the spectrum in this region. Our data prevent an estimate at 1.558 μm, but Volk et al. (2003) report a difference of 1.3 mag. In addition, the position angle is at 35° to the 0.″35 slit. Detailed examination of the spectral images showed no trace of ϵ Ind Bb at the location expected, so we are confident that our spectra are contributed almost entirely by ϵ Ind Ba.

Each program star was observed along the slit at two or three separate positions separated by 4″–5″ on the sky: the delivered image FWHM at the spectrograph varied from 0.″25 to 0.″80 during the nights that spectra were taken, so stellar images at different positions on the slit were well separated on the detector. Equal integration times were used for a particular program star during a particular set of observations. With this observing strategy, sky and dark backgrounds are removed by subtracting one integration from another (the star being at different positions on the detector array). During each night, 10 flat-field and 10 dark images were recorded for each given wavelength setting of the echelle. A hot star, with no intrinsic spectral lines in the regions observed, was also observed each night in each observed wavelength region.

Two-dimensional images were reduced to one-dimensional spectra using an optimal extraction algorithm described in Johns-Krull, Valenti, & Koresco (1999). Wavelengths and telluric corrections in the 2.31 μm region were determined by fitting observed telluric features with a scaled atmospheric transmission function from Wallace & Hinkle (2001). There are no significant telluric features in the 1.56 μm region, so the wavelength scale was determined by matching a spectrum of HR 1629 (K4 III) with an IR Fourier transform spectroscopic atlas of Arcturus (Hinkle, Wallace, & Livingston 1995)

Figure 1 illustrates the combined and reduced spectra for ϵ Ind Ba in both the 2.313 and 1.556 μm regions, with the wavelengths plotted as air wavelengths. The data points have been smoothed over the slit width of 4 pixels, and the final signal-to-noise ratio is about 30–40. The 2.31 μm region contains strong vibration-rotation lines from the first overtone bands of CO [here (2–0) lines from $^{12}C^{16}O$], as well as some weak, blended H_2O features, and weak absorption from methane. Detectable spectral

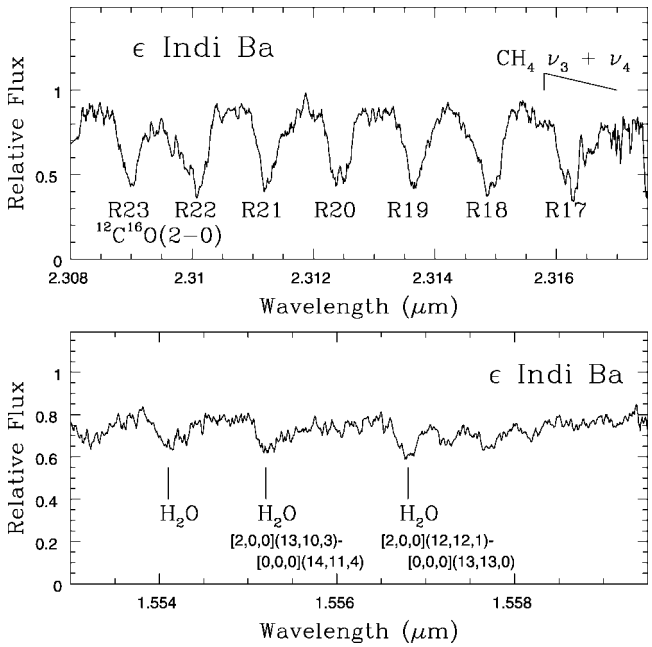

FIG. 1.—λ2.313 μm (*top*) and λ1.556 μm (*bottom*) spectra of ϵ Ind Ba, with the plotted wavelengths being those in air. The 2.31 μm region is dominated by strong $^{12}C^{16}O$ (2–0) lines that are rotationally broadened. The CH_4 absorption at λ2.318 μm is either absent or very weak at this high spectral resolution. The 1.55 μm region exhibits blended features from H_2O.

features at 1.55 μm are not as strong as at 2.31 μm nor as well defined as the individual vibration-rotation CO lines and consist mostly of blended H_2O features. Two of the stronger features can be assigned to mainly two H_2O lines (as marked in Fig. 1) on the basis of the study of H_2O by Tereszchuk et al. (2002).

3. ANALYSIS AND DISCUSSION

The observed spectra of ϵ Ind Ba at 2.313 and 1.556 μm are compared to synthetic spectra calculated from model atmospheres as discussed by Tsuji (2002). These models are so-called unified cloudy models, in which dust is allowed to exist in the photosphere over a limited range defined by a condensation temperature, $T_{\rm cond}$, and a critical temperature, $T_{\rm cr}$, such that dust is found in the region of $T_{\rm cr} \le T \le T_{\rm cond}$. At the critical temperature, dust grains become so large that they precipitate from the the photosphere. The models employed in this analysis are computed with plane parallel geometry, in hydrostatic equilibrium, and have solar abundances.

Figure 2 illustrates a comparison of observed and synthetic spectra, for both the 2.313 μm (*top*) and 1.556 μm (*bottom*) regions. The 2.313 μm spectrum contains strong $^{12}C^{16}O$ (2–0) lines and some weak H_2O features. The 1.556 μm spectrum exhibits primarily H_2O absorption, with these features composed of many blended individual spectral lines. In the top panel, the comparison synthetic spectra span effective temperatures from 1400 to 1800 K, and these models have surface gravities of $\log g = 5.5$ (in units of cm s^{-2}). This particular spectral region is illustrated as any CH_4 absorption beginning near $\lambda \sim 2.3158$ μm and, clearly apparent in the models with $T_{\rm eff} = 1400$ or 1500 K, is very temperature sensitive. Its observed absence (or extreme weakness) in ϵ Ind Ba indicates that $T_{\rm eff} = 1600$ K; higher effective temperatures begin to produce CO lines that are too weak. The CO lines that dominate this region are not very sensitive to gravity over the expected range for the brown dwarfs with these approximate tempera-

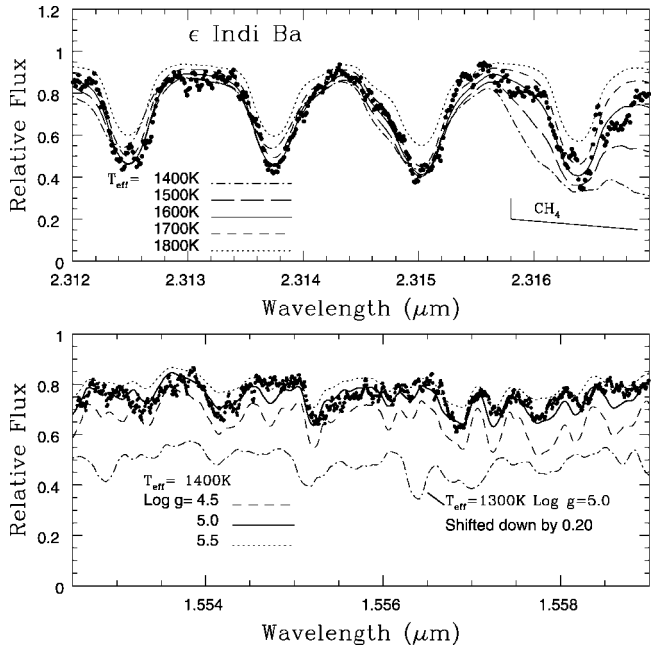

FIG. 2.—Comparison of the observed spectra of ϵ Ind Ba with synthetic spectra that span a range of effective temperatures and gravities. *Top*: The $\lambda 2.314$ μm region is shown, with the strong $^{12}C^{16}O$ lines, as indicated in Fig. 1. In order to fit the observed line shapes, the model spectra must be broadened by a rotational profile with $v_{rot} = 28$ km s^{-1}. This spectral region is illustrated because of the large temperature sensitivity of the CH_4 absorption (as well as the CO). A good fit is obtained for $T_{eff} = 1600$ K. These particular lines are not very sensitive to gravity over the expected values, so a single-gravity set of models is shown (with $\log g = 5.5$). *Bottom*: Observed and model spectra comparisons are shown for a single $T_{eff} = 1400$ K but a range of gravities. Most of the blended spectral features visible in this wavelength region are from H_2O, and the relative depth of the absorption is sensitive to gravity, as illustrated. Surface gravities in the range of $\log g = 5.0$–5.5 are the overall best fits. Note that higher effective temperatures will produce extremely weak H_2O absorption, while lower T_{eff} result in increasingly dominant CH_4 absorption, which is not observed. The vertically shifted model spectrum is for $T_{eff} = 1300$ K and illustrates the increasingly different absorption as the temperature decreases (note the strong feature at 1.5564 μm from CH_4.

tures; however, the 1.556 μm region features dominated by H_2O are more sensitive to surface gravity, as shown in the bottom panel of Figure 2. Here a slightly lower effective temperature is derived, with $T_{eff} = 1400$ K, and the gravity-sensitive H_2O features indicate that $\log g \sim 5.0$–5.5. Higher effective temperatures produce H_2O absorption features that are too weak for any reasonable surface gravity, while temperatures much lower than $T_{eff} = 1400$ K (say, 1300 K) produce increasingly strong CH_4 absorption, which looks nothing like the observed spectrum of ϵ Ind Ba. This effect is shown by the $T_{eff} = 1300$ K model spectrum in the bottom panel of Figure 2 that is offset vertically from the observed spectra and 1400 K models. The offset is done as the different absorption features in the 1300 K model (that are caused by increasing CH_4 and decreasing H_2O absorption), if overlaid on the observed spectrum, would produce merely confusion.

Fits to the line profiles (primarily the strong CO lines), as shown in Figure 2, also yield the projected rotational velocity, with $v \sin i = 28$ km s^{-1} (with an uncertainty of ± 3 km s^{-1}). Wavelength shifts between observed and synthetic spectra also provide an accurate radial velocity for ϵ Ind Ba, which we find to be $V_{helio} = -41.0 \pm 0.7$ km s^{-1}. This radial velocity is very close to the published value for ϵ Ind A's velocity of -39.6 ± 0.8 km s^{-1} from Wielen et al. (1999). The similarity of radial velocities for both ϵ Ind A and Ba strengthens their physical association, as argued by Scholz et al. (2003), based on their respective distances and proper motions.

The combination of both the 2.314 and 1.555 μm high-resolution spectra and their comparison to synthetic spectra result in values for temperature and gravity in ϵ Ind Ba to be $T_{eff} = 1400$–1600 K and $\log g = 5.0$–5.5. Taking the average of these values as being the best estimates, we find an effective temperature of 1500 K and a gravity of $\log g = 5.25$. McCaughrean et al. (2003) used photometry to derive the luminosity of ϵ Ind Ba and found it to be $\log (L/L_{\odot}) = -4.71$. This luminosity can be combined with our estimates of temperature and gravity to yield a spectroscopic mass estimate of $30M_J$. McCaughrean et al. (2003) derive a mass of $40M_J$–$60M_J$, which is close to the mass derived from the high-resolution spectra. In addition, given the luminosity and effective temperature, the radius of ϵ Ind Ba can be estimated and then combined with the projected rotational velocity to yield a maximum rotational period. With $\log (L/L_{\odot}) = -4.71$ and $T_{eff} = 1500$ K, a radius of $(R/R_{\odot}) = 0.062$ is derived. Given $v \sin i = 28$ km s^{-1}, the maximum rotational period for ϵ Ind Ba will be 3.0 hr.

The effective temperature derived by McCaughrean et al. (2003) is 1275 K and results from the luminosity combined with the distance and a radius defined by a theoretical M_{bol}-radius relation that results from structural models of brown dwarfs. This T_{eff} is somewhat lower than our value of 1500 K; however, this difference is typical of the differences found to date between spectroscopically derived effective temperatures and those derived from structural models. The differences in T_{eff} also indicate differences in the implied radii from the two methods. In our case, the higher spectroscopic T_{eff} for ϵ Ind Ba requires a smaller radius to support its luminosity. The two techniques are complementary in the sense that the radius does not enter into the computation of the plane parallel atmosphere but does in the M_{bol}-radius relation. Age uncertainties can also affect derived physical paprameters, especially for the structural models. Larger sets of comparison measurements of physical parameters derived from both model atmospheres and structural models will improve our understanding of the root cause of these differences. A comparison of the temperature scales is illustrated in Figure 3, where spectroscopic T_{eff} are plotted versus structural T_{eff}; the spectroscopic temperatures are taken from Basri et al. (2000), Leggett et al. (2001), and Schweitzer et al. (2002), while the structural temperatures are those from Dahn et al. (2002). The Dahn et al. T_{eff}'s also use a M_{bol}-radius relation from structural models in deriving temperatures. Despite using different sets of model atmospheres (with differing treatments of dust), there is a clear trend in the differences between the spectroscopically derived effective temperatures when compared to the structural temperatures from Dahn et al. (2002). At higher temperatures, the spectroscopic T_{eff}'s tend to fall below the structural T_{eff}'s, with the reverse situation at lower temperatures and a crossover point at ~1900–2000 K. Our derived T_{eff} for ϵ Ind Ba falls nicely on the cool end of this trend. We do not speculate here on the reasons for the systematic differences between structural and spectroscopic effective temperatures.

The treatment of dust in the photosphere is a crucial ingredient in the quantitative spectral modeling of the cool L and T dwarfs. Here we have used the unified dust models, as discussed in detail by Tsuji (2002); however, we also investigated other dust treatments to see what effects these would have on the derived physical parameters (primarily T_{eff}). Two other sets of model atmospheres were generated: (1) one in which dust

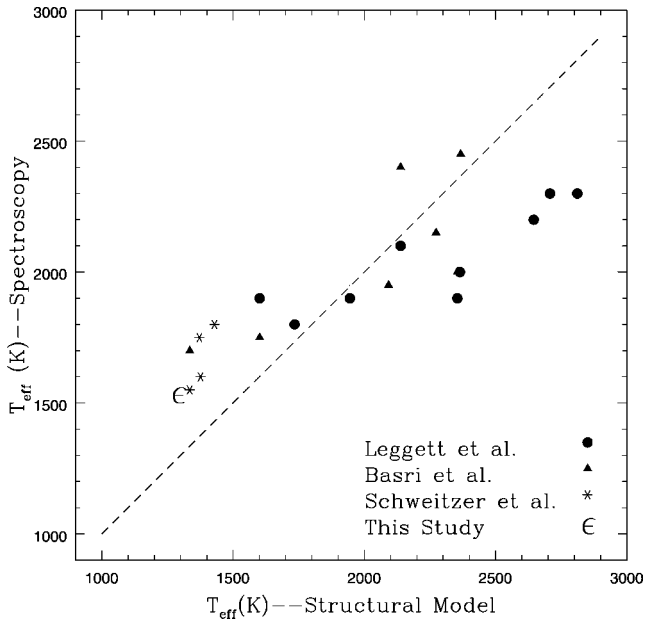

FIG. 3.—Comparison of effective temperatures derived from model atmosphere spectrum synthesis techniques to temperatures derived from structural models for L and T dwarfs. The structural T_{eff} are taken from Dahn et al. (2002), while the spectroscopic temperatures are from Basri et al. (2000), Leggett et al. (2001), and Schweitzer et al. (2002). There is a well-defined systematic trend in the differences between spectroscopic and structural effective temperatures, with our result for ϵ Ind Ba falling at the cool end of this trend.

remained in all layers where the thermochemical conditions allowed dust condensation (case B) and (2) the other being the case in which all dust sank out of the photospheric layers (case C). These very same effects were also investigated and discussed in detail by Basri et al. (2000) for a sample of late M and L dwarfs. In our case B, where dust exists over a wide range of depths in the photosphere, the model absorption lines (CO, H_2O, and CH_4) are all much weaker than the observed absorption lines (the addition of significant dust opacity over a large region of the photosphere weakens the gas phase absorption lines), and no realistic fit to the observed spectra is possible for any reasonable T_{eff}. For the atmospheres where all dust sinks from the photosphere (case C), the model molecular absoprtion lines have more realistic strengths, but the temperature-sensitive CH_4 appears at even higher effective temperatures; we derive $T_{eff} = 1800$ K for ϵ Ind Ba. The disagreement with the structural models is even worse here. This exercise suggests that some dust in the photosphere provides a better physical picture in modeling the high-resolution IR spectra of ϵ Ind Ba. Our initial comparison here points to the need for more high-resolution spectral analyses across the temperature range of the L and T dwarfs.

4. CONCLUSIONS

We have used high-resolution IR spectra of the nearest brown dwarf, ϵ Ind Ba, to derive its physical parameters using comparisons to synthetic spectra calculated from model atmospheres. The spectroscopic $T_{eff} = 1500$ K, with $\log g = 5.2$, and an estimated mass of $M = 30 M_J$. The projected rotational velocity is $v \sin i = 28$ km s^{-1}, indicating a maximum rotational period of ~3.0 hr. The comparison between the T_{eff} scales derived from spectroscopic plus model atmosphere analyses against those derived from M_{bol}-radius relations reveals a significant systematic difference that is unexplained.

The staff of the Gemini South Observatory are to be thanked for technical support. We also thank J. Tennyson for his comments on the H_2O assignments and the referee (G. Basri) for helpful suggestions in improving this paper. This research had made use of the SIMBAD database, operated at CDS, Strasbourg, France. The work reported here is supported in part by the National Science Foundation through AST 99-87374 (V. V. S.) and NASA through NAG5-9213 (V. V. S.).

REFERENCES

Basri, G., Mohanty, S., Allard, F., Hauschildt, P. H., Delfosse, X., Martín, E. L., Forveille, T., & Goldman, B. 2000, ApJ, 538, 363
Dahn, C. C., et al. 2002, AJ, 124, 1170
Geballe, T. R., et al. 2002, ApJ, 564, 466
Hinkle, K. H., Cuberly, R., Gaughan, N., Heynssens, J., Joyce, R., Ridgway, S., Schmitt, P., & Simmons, J. E. 1998, Proc. SPIE, 3354, 810
Hinkle, K. H., Wallace, L., & Livingston, W. 1995, PASP, 107, 1042
Johns-Krull, C. M., Valenti, J. A., & Koresco, C. 1999, ApJ, 516, 900
Kirkpatrick, J. D., et al. 1999, ApJ, 519, 802
Lachaume, R., Dominik, C., Lanz, T., & Habing, H. J. 1999, A&A, 348, 897
Leggett, S. K., Allard, F., Geballe, T. R., Hauschildt, P. H., & Schweitzer, A. 2001, ApJ, 548, 908
McCaughrean, M. J., Close, L. M., Scholz, R.-D., Lenzen, R., Biller, B., Brandner, W., Hartung, M., & Lodieu, N. 2003, A&A, in press (astro-ph/0309256)
Scholz, R. D., McCaughrean, M. J., Lodieu, N., & Kuhlbrodt, B. 2003, A&A, 398, L29
Schweitzer, A., Gizis, J. E., Hauschildt, P. H., Allard, F., Howard, E. M., & Kirkpatrick, J. D. 2002, ApJ, 566, 435
Tereszchuk, K., Bernath, P. F., Zobov, N. I., Shirin, S. V., Polyansky, O. L., Libeskind, N., Tennyson, J., & Wallace, L. 2002, ApJ, 577, 496
Tsuji, T. 2002, ApJ, 575, 264
Volk, K., Blum, R., Walker, G., & Puxley, P. 2003, IAU Circ. 8188
Wallace, L., & Hinkle, K. 2001, Sunspot Umbral Spectra in the Region 4000–8640 cm^{-1} (1.16–2.50 μm), NSO Tech. Rep. 01-001 (Tucson: NSO)
Wielen, R., Schwan, H., Dettbarn, C., Lenhardt, H., Jahreiss, H., & Jahrling, R. 1999, Veröff. Astron. Rechen-Inst. Heidelberg, 35, 1